

Contents lists available at GrowingScience

## Current Chemistry Letters

homepage: www.GrowingScience.com

## Nonlinear optical response of D- $\pi$ -A chromophores based on benzoxazin: quantum modification of $\pi$ -spacer

A. Azaid<sup>a</sup>, T. Abram<sup>a</sup>, R. Kacimi<sup>a</sup>, M. Raftani<sup>a</sup>, Y. Khaddam<sup>a</sup>, D. Nebbach<sup>a</sup>, A. Sbai<sup>a</sup>, T. Lakhli<sup>a</sup> and M. Bouachrine<sup>a,b\*</sup>

<sup>a</sup>Molecular chemistry and Natural Substances Laboratory, Faculty of Science, University Moulay Ismail, Meknes, Morocco

<sup>b</sup>Superior School of Technology - Khenifra (EST-Khenifra), University of Sultan My Slimane, PB 170, Khenifra 54000 Morocco

### CHRONICLE

#### Article history:

Received August 22, 2021

Received in revised form

October 25, 2021

Accepted February 22, 2022

Available online

February 22, 2022

#### Keywords:

Benzoxazine

Tricyanovinyl dihydrofuran

(TCF)

NLO

TD-DFT

NBO

### ABSTRACT

In this research article, four chromophores based on benzoxazine as the electron donor and tricyanovinyl dihydrofuran (TCF) as the electron acceptor have been designed to investigate the nonlinear optical (NLO) response. The geometric and electronic structures, absorption spectra, NBO analysis, and nonlinear optical response have been calculated by employing density functional theory (DFT) at PBEPBE/6-31G (*d,p*). The new design of chromophores has been proposed by the structural modification of  $\pi$ -spacers/conjugated systems. The DFT and TD-DFT computations at CAM-B3LYP/6-31G (*d,p*) have been performed to shed light on the influences of structural modification on the NLO properties. The absorption wavelength in different organic solvents, polarizability ( $\alpha$ ), and hyperpolarizability ( $\beta$ ) are all determined. A strong NLO response indicates that this family of organic compounds with a D- $\pi$ -A structure exhibits large first hyperpolarizability  $\beta_{tot}$  values, these values are much greater than ones of urea. This theoretical model may be used to design other chromophores for usage in electro-optics.

© 2022 by the authors; licensee Growing Science, Canada.

## 1. Introduction

Over the past decade, organic compounds have attracted considerable attention due to ease of synthesis and fabrication, low cost, and their potential applications in novel optoelectronic devices for telecommunications, optical bistability, information storage, high-speed all-optical switches, and signal processing.<sup>1-3</sup> Indeed, the ease of modifying organic molecules structurally enables researchers to control the chemical structures and characteristics of desired nonlinear optical (NLO) responses.<sup>4</sup> These molecules with delocalized electrons are getting more attention due to their strong nonlinear optical characteristics. It has been determined that the characteristics of second-order nonlinear optical/first hyperpolarizability are related to intramolecular charge transfer (CT).<sup>5</sup> The charge transfer occurs between the donor and the acceptor via the  $\pi$ -spacer.<sup>6,7</sup> The NLO characteristics of basic molecules ascertain the NLO properties of the organic material. This criterion helps in the modeling of organic molecules with high NLO values.<sup>8</sup> To simulate and construct high-response NLO materials, it is necessary to modify the conjugation and therefore, the NLO activity of the materials.<sup>9</sup> The literature shows that donor and acceptor groups are responsible for supplying the essential ground-state charge asymmetry and the  $\pi$ -conjugated system offers a channel for the transfer and distribution of electric charges under the application of an electric field.<sup>10</sup> Generally, the D- $\pi$ -A structure is developed to promote CT transitions. This structure enables us to investigate the influence of donor and acceptor group strengths, as well as the nature and the degree of  $\pi$ -conjugation on the functions of the nonlinear optical response. According to the structure-property relationship, the  $\beta$  value increases when the length of the  $\pi$ -conjugating chain is lengthened.<sup>11-13</sup>

\* Corresponding author.

E-mail address: [m.bouachrine@est-umi.ac.ma](mailto:m.bouachrine@est-umi.ac.ma) (M. Bouachrine)

© 2022 by the authors; licensee Growing Science, Canada

doi: 10.5267/j.ccl.2022.3.001

Recently, a new chromophore Z1 with the structure D- $\pi$ -A was successfully prepared by Haoran Wang et al.<sup>14</sup> This chromophore contains benzoxazine as the electron donor, thiophene as the  $\pi$ -conjugated bridge, and tricyanovinyl dihydrofuran (TCF) as the electron acceptor Fig. 1. This chromophore was proposed for nonlinear optical (NLO) applications.

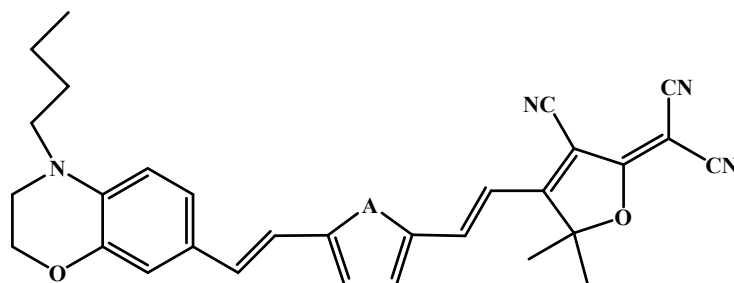


Fig. 1. Structure of chromophore Z1

The purpose of this work is to determine the influence of the length of conjugation on the NLO characteristics and UV-visible spectra of the organic chromophores. Indeed, large second-order NLO responses were simulated using the strategy of modifying organic molecules by lengthening the conjugated bridge. Four organic chromophores (Z1-Z4) with varying  $\pi$ -spacers were investigated. The structure of these four compounds is shown in fig. 2. Quantum chemical calculations were performed to compute the geometric and electronic structures, NBO analysis, nonlinear optical response, and absorption spectra of all compounds studied. We believe that our research will aid in the design and development of effective NLO organic chromophores in future experiments. Additionally, this work will aid experimentalists in developing more efficient NLO materials.

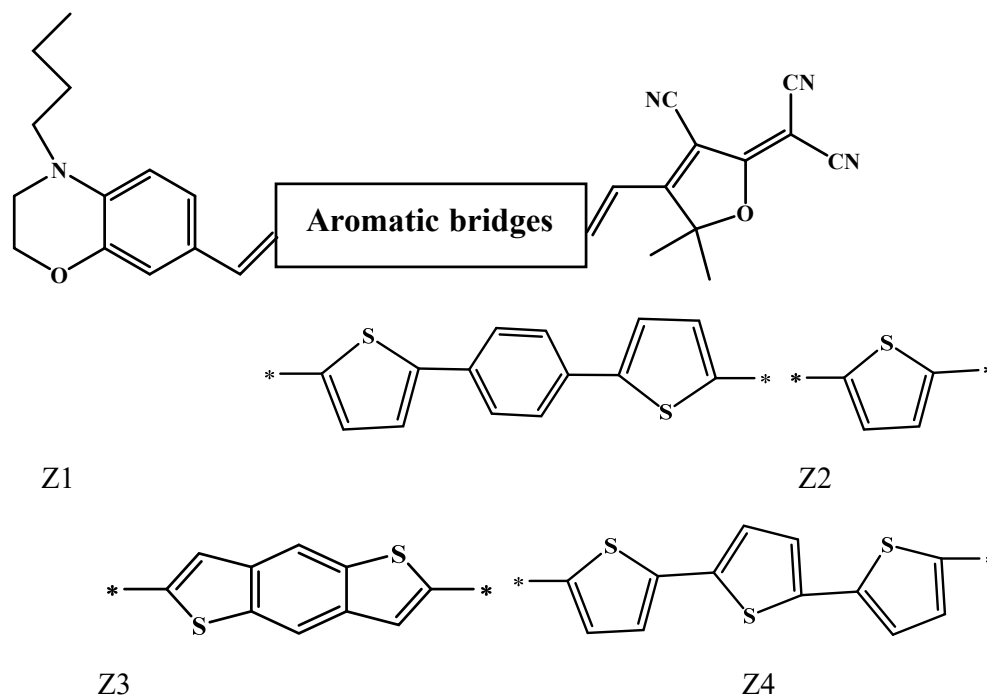


Fig. 2. Structures of chromophores Z1-Z4

## 2. Materials and methods

The hybrid functionals B3LYP,<sup>15,16</sup> PBEPBE,<sup>17</sup> B3PW91,<sup>18</sup> and mPW1PW9<sup>19</sup> were employed in this study. All computations are performed using the 6-31G (*d,p*) basis set.<sup>20,21</sup> The density functional theory (DFT) and time-dependent DFT computations were carried out using the Gaussian 09 software.<sup>22</sup> Organic chromophores structures were optimized in the gas phase, and the HOMO, LUMO, and Egap energies were determined.<sup>23-25</sup> The computed orbital populations were used to forecast the natural bond orbital (NBO)<sup>26</sup> analysis using the NBO 6.0 software incorporated into the Gaussian 09 package program. For designed molecules, the spectrum of absorption, vertical absorption energies, and oscillator strengths was calculated in different organic solvents using the Time-Dependent Density Functional Theory (TD-DFT)<sup>27</sup> with coulomb-attenuated hybrid exchange-correlation functional (CAM-B3LYP).<sup>28</sup> Furthermore, we used DFT with the PBEPBE functional and the basis set 6-31G (*d,p*) to analyze NLO properties for molecules Z1, Z2, Z3 and Z4, such as the

first hyperpolarizability ( $\beta_{tot}$ ) and their related parameters ( $\mu, \alpha$ ). Indeed, the total dipole moment ( $\mu$ ), the mean polarizability ( $\alpha$ ), and the first hyperpolarizability ( $\beta_{tot}$ ) are all characteristics that suggest their usefulness as nonlinear optical materials.<sup>29-31</sup>

They are calculated using the x, y, and z units in equations (1) – (3):

Here, combines the different quantities:

$$\mu_{tot} = \sqrt{\mu_x^2 + \mu_y^2 + \mu_z^2} \quad (1)$$

$$\langle \alpha \rangle = \frac{1}{3}(\alpha_{xx} + \alpha_{yy} + \alpha_{zz}) \quad (2)$$

$$\beta_{tot} = \sqrt{\beta_x^2 + \beta_y^2 + \beta_z^2} \quad (3)$$

Here,  $\beta_i = (i = x, y, z)$  combines the different quantities:  $\beta_i = (\frac{1}{3})\sum_{j=x,y,z}(\beta_{ijj} + \beta_{jij} + \beta_{jji})$ .

### 3. Results and discussion

#### 3.1 Choice of methods

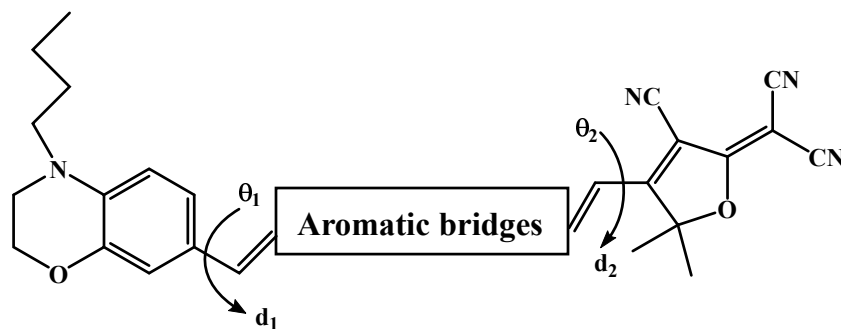
The selection of the functional using DFT approach is essential to properly explain the electronic properties ( $E_{HOMO}$ ,  $E_{LUMO}$ ,  $E_{gap}$ ) of the chromophore studied.<sup>14</sup> Particularly, B3LYP, PBEPBE, B3PW91, and mPW1PW91 with the same basis set 6-31G (*d,p*) has been used in this regard. The results of the four functional groups applied for the reference chromophore Z1 are listed in **Table 1**. We observe that the energy gap obtained by the PBEPBE functional with 6-31G (*d,p*) level is similar to that obtained experimentally with a tolerable margin of error. Furthermore, the energy gap ( $E_{gap}$ ) values obtained by the B3LYP, B3PW91, and mPW1PW91 functionals are larger than those determined experimentally. As a result, we conclude that PBEPBE is a great suited for describing the electronic characteristics and the ground-state geometries of all our organic chromophores.

**Table 1.** Energies of HOMO, LUMO, and the gap energy for Z1 chromophore obtained by DFT/6-31G (*d,p*) with different functional levels, compared with those obtained experimentally.

| Functionals     | Chromophore Z1  |                 |                        |                  |                           |
|-----------------|-----------------|-----------------|------------------------|------------------|---------------------------|
|                 | $E_{HOMO}$ (eV) | $E_{LUMO}$ (eV) | $E_g$ theoretical (eV) | $E_{g,exp}$ (eV) | $\Delta E_{(Error)}$ (eV) |
| <b>B3LYP</b>    | -5.213          | -3.125          | 2.08                   |                  | 0.77                      |
| <b>B3PW91</b>   | -5.311          | -3.225          | 2.08                   |                  | 0.77                      |
| <b>mPW1PW91</b> | -5.447          | -3.100          | 2.34                   | 1.31             | 1.03                      |
| <b>PBEPBE</b>   | -4.656          | -3.505          | 1.15                   |                  | 0.16                      |

#### 3.2 Optimized ground-state geometries

All optimized geometries of the (Z1-Z4) chromophores obtained by DFT/PBEPBE with 6-31G (*d,p*) levels are shown in **Fig. 3**. The primary optimization geometrical parameters such as bond lengths and dihedral angles are listed in Table 2.



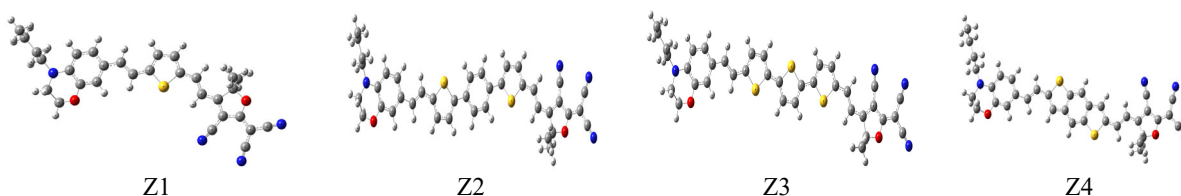
**Scheme 1.** Studied geometric parameters

According to **Scheme 1**,  $d_1$  and  $d_2$ , represent the bond length obtained between benzoxazine as the electron donor (D) and the  $\pi$ -spacer and between the tricyanovinyl dihydrofuran (TCF) as the electron acceptor (A) and the same  $\pi$ -spacer, respectively. Based on data in **Table 2**, The shortest values estimated lengths  $d_1$  and  $d_2$  for all organic chromophores are in the range of 1.42 Å to 1.45 Å, indicating a C=C character that confirms and simplifies intramolecular charge transfer ICT,<sup>32</sup> this affects the redshift of the absorption spectrum.<sup>33</sup> For dihedral angles, the values of  $\theta_1$  produced by the benzoxazine

moiety and the  $\pi$ -spacer for all designed molecules (Z1-Z4) are  $179.85^\circ$ ,  $177.86^\circ$ ,  $178.80^\circ$ , and  $-178.94^\circ$ , respectively. Additionally, the dihedral angles  $\theta_2$  created by the acceptor group and the  $\pi$ -spacer of all compounds (Z1-Z4) are  $-179.71^\circ$ ,  $-179.72^\circ$ ,  $179.82^\circ$ , and  $-178.83^\circ$ , respectively. Indeed, the results obtained for  $\theta_1$  and  $\theta_2$  indicate that all the chromophores proposed have a planar conformation.

**Table 2.** Distances ( $\text{\AA}$ ) and dihedral angles  $\theta_i$  ( $^\circ$ ) of the studied chromophores calculated by PBEPBE/6-31G (*d,p*)

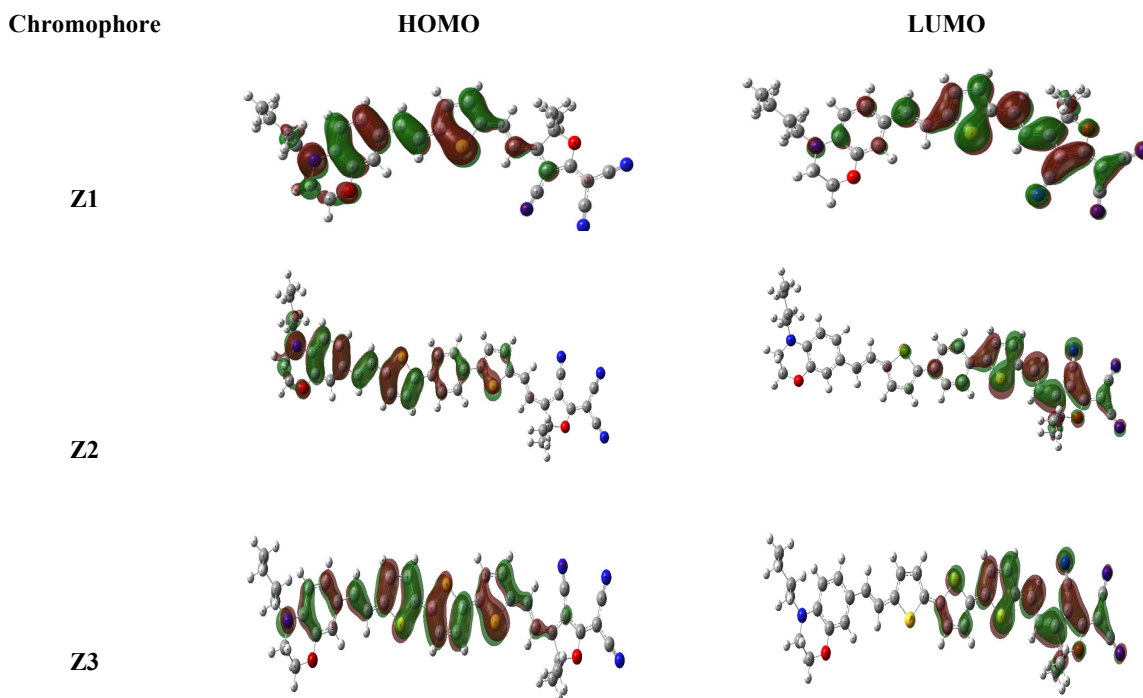
| Chromophore | d1( $\text{\AA}$ ) | d2( $\text{\AA}$ ) | $\theta_1$ ( $^\circ$ ) | $\theta_2$ ( $^\circ$ ) |
|-------------|--------------------|--------------------|-------------------------|-------------------------|
| Z1          | 1.42               | 1.45               | 179.85                  | -179.71                 |
| Z2          | 1.42               | 1.45               | 177.86                  | -179.72                 |
| Z3          | 1.42               | 1.45               | 178.80                  | 179.82                  |
| Z4          | 1.42               | 1.45               | -178.94                 | -178.83                 |



**Fig. 3.** Optimized structures of all studied chromophores (Z1-Z4) using PBEPBE/6-31G (*d,p*) level

### 3.3 Molecular orbitals

To understand more about intramolecular charge transfer (ICT), the electronic distributions of molecular orbital frontiers of four chromophores were computed using the PBEPBE functional with 6-31G (*d,p*) level, which is represented in **Fig. 4**. From the obtained results, the electronic distribution of the HOMO of Z1, Z2, and Z3 are mainly distributed on the donor and the  $\pi$ -bridge, while Z4 is predominantly delocalized on the  $\pi$ -bridge. On the other hand, the LUMO of all chromophores (Z1-Z4) shows a distribution on the  $\pi$ -bridge and acceptor groups. Accordingly, absorption occurs when an electron transitions from the HOMO to the LUMO level. In this context, chromophores with a smaller energy band gap are more conducive to electron excitations, which improves the absorption properties of the chromophores. Therefore, the energy gap ( $E_{\text{gap}}$ ) of all studied chromophores was calculated according to the following relation:  $E_{\text{gap}} = E_{\text{HOMO}} - E_{\text{LUMO}}$ <sup>33</sup> and is listed in Table 3. According to this table, the gap energy for Z1 is 1.15 eV, which is in excellent agreement with the experimental measurement (1.31 eV).<sup>18</sup> In comparison to Z1, the gap energy decreases in the following order: Z1 (2.09 eV) > Z4 (0.90 eV) > Z3 (0.85 eV) > Z2 (0.79 eV).



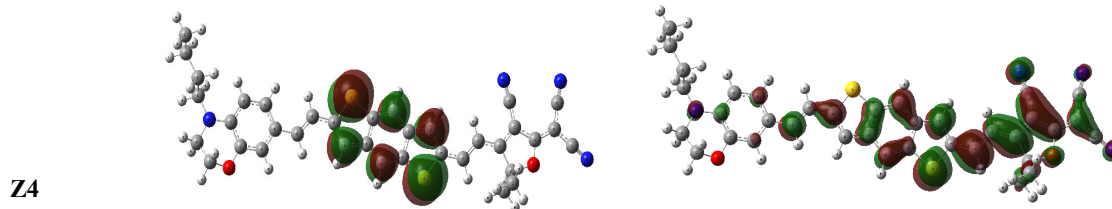


**Fig. 4.** Contour plots of the frontier orbitals of all chromophores

**Table 3.** Energy values in eV of HOMO ( $E_{\text{HOMO}}$ ), LUMO ( $E_{\text{LUMO}}$ ) and gap ( $E_{\text{gap}}$ ) of all studied chromophores.

| Chromophore | $E_{\text{HOMO}}$ (eV) | $E_{\text{LUMO}}$ (eV) | $E_{\text{gap}}$ (eV) |
|-------------|------------------------|------------------------|-----------------------|
| Z1          | -4.656                 | -3.505                 | 1.15                  |
| Z2          | -4.405                 | -3.613                 | 0.79                  |
| Z3          | -4.443                 | -3.593                 | 0.85                  |
| Z4          | -4.543                 | -3.643                 | 0.90                  |

### 3.4 NBO analysis

The NBO study is an excellent method for exploring charge transfer between the occupied and unoccupied orbitals, and it is an efficient technique to investigate the ICT. NBO analysis is also believed to be able to show the charge densities that transfer from a donor group to an acceptor group via a  $\pi$ -linker in the D- $\pi$ -A architecture. Therefore, NBO analysis of optimized structures of Z1-Z4 chromophores has been performed using the DFT-PBEPBE/6-31G (*d,p*) method in the gas phase, and the calculated data are shown in **Table 4**.<sup>34</sup> It is important to note that all compounds have positive charges in the donor and  $\pi$ -spacer groups, whereas the acceptor group has negative charges. On the other hand, the positive charges in the inserted bridge reveal that this unit functions as a donor. The highest positive charge on the donor of the chromophores Z1 and Z4 and the  $\pi$ -spacer for all chromophores indicates the most effective electron donor, while the most negative (NBO) charge on the acceptor portion indicates the best acceptor group for all chromophores investigated. These findings indicate that electrons migrate effectively from the donor to the acceptor groups through  $\pi$ -conjugated linkers, this corresponds to the formation of a state of charge separation.

**Table 4.** The NBO analysis of all chromophores (Z1-Z4) obtained at DFT/ PBEPBE/6-31G (*d,p*) level

| Compound | Donating Group | $\pi$ - spacer | Acceptor Group |
|----------|----------------|----------------|----------------|
| Z1       | 0.145          | 0.121          | -0.266         |
| Z2       | 0.096          | 0.169          | -0.265         |
| Z3       | 0.093          | 0.167          | -2.260         |
| Z4       | 0.131          | 0.112          | -0.243         |

### 3.5 Molecular electrostatic potential (MEP)

The electron density is an essential factor for determining both the reactivity of electrophilic and nucleophilic sites, as well as the interactions of hydrogen bonding. It is also associated with the molecule electrostatic potential (MEP).<sup>35</sup> In order to assess the reactivity of nucleophilic and electrophilic site attacks of the investigated chromophores, we predicted the MEP of these compounds by applying DFT / PBEPBE / 6-31G (*d,p*) approaches on the optimized geometry. The map of the MEP surface is given in **Fig. 5** using a variety of colors. As seen in **Fig 5**, the MEP demonstrates that the maximum positive region (blue color) of all chromophores is around the sulfur atoms of the  $\pi$ -spacer fragment. Whereas the negative region (red color) is predominantly concentrated around the nitrogen atoms of the tricyanovinyl dihydrofuran (TCF) groups in all investigated chromophores.

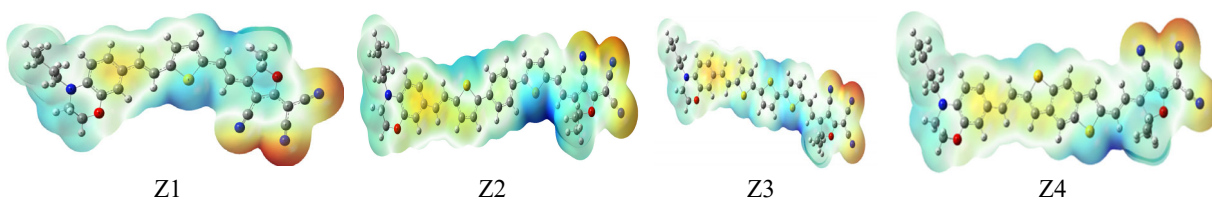


**Fig. 5.** MEP surfaces of the four studied compounds

### 3.6 Chemical concepts of reactivity

The DFT method is a very useful framework for the study of chemical reactivity. It offers information on the electronic structure of chemical species.<sup>36</sup> Using the HOMO and LUMO energies ( $E_{\text{HOMO}}$  and  $E_{\text{LUMO}}$ ), the chemical potential ( $\mu$ ),<sup>37</sup> chemical hardness ( $\eta$ ),<sup>38,39</sup> softness ( $S$ ) and electronegativity ( $\chi$ )<sup>40</sup> are all computed for the chromophores listed in **Table 5**. These Chemical reactivity indices may be determined using the following formulae:

$$\text{Chemical hardness: } \eta = \frac{E_{\text{LUMO}} - E_{\text{HOMO}}}{2} \quad (4)$$

$$\text{Chemical potential: } \mu = \frac{E_{\text{LUMO}} + E_{\text{HOMO}}}{2} \quad (5)$$

$$\text{Electronegativity: } \chi = -\mu = \frac{-(E_{\text{LUMO}} + E_{\text{HOMO}})}{2} \quad (6)$$

$$\text{Chemical softness: } S = \frac{1}{2\eta} = \frac{1}{E_{\text{LUMO}} - E_{\text{HOMO}}} \quad (7)$$

As shown in **Table 5**, the electronic chemical potential ( $\mu$ ) of four studied chromophore increases in the following order: Z4 (-4.09) < Z1 (-4.08) < Z3 (-4.02) (eV) < Z2 (-4.01) (eV). The values of hardness ( $\eta$ ) show that the compounds Z1, Z2, Z3 and Z4 have the lowest hardness values, i.e., 0.57, 0.39, 0.42 and 0.45 (eV), respectively. Hence, they are soft molecules. In addition, the electronegativity ( $\chi$ ) values of the compounds Z1-Z4 were found to be 4.08, 4.01, 4.02 and 3.99 (eV), respectively. Finally, the values of softness (S) for all the investigated compounds increase in the following order: Z1 (0.87) < Z4 (1.11) < Z3 (1.19) (eV) < Z2 (1.28) (eV).

**Table 5.** HOMO, LUMO, and gap energies, chemical potential ( $\mu$ ), chemical hardness ( $\eta$ ), chemical softness (S), and electronegativity ( $\chi$ )

| Chromophore | $E_{\text{HOMO}}$ (eV) | $E_{\text{LUMO}}$ (eV) | $E_{\text{gap}}$ (eV) | $\mu$ | $\eta$ | S    | $\chi$ |
|-------------|------------------------|------------------------|-----------------------|-------|--------|------|--------|
| Z1          | -4.656                 | -3.505                 | 1.15                  | -4.08 | 0.57   | 0.87 | 4.08   |
| Z2          | -4.405                 | -3.613                 | 0.79                  | -4.01 | 0.39   | 1.28 | 4.01   |
| Z3          | -4.443                 | -3.593                 | 0.85                  | -4.02 | 0.42   | 1.19 | 4.02   |
| Z4          | -4.543                 | -3.643                 | 0.90                  | -4.09 | 0.45   | 1.11 | 4.09   |

### 3.7 Nonlinear optical (NLO) properties

The nonlinear optical (NLO) responses are intriguing in a variety of domains, including electro-optics and data storage.<sup>41</sup> Indeed, the molecular structure, which contains the appropriate donor and acceptor groups in the strategic positions is the primary characteristic of NLO, which may be further modified by extending  $\pi$ -conjugation.<sup>42,43</sup> To verify their utility as NLO materials, NLO parameters of the studied chromophores (Z1-Z4) have been estimated using the PBEPBE theory and the 6-31G (*d,p*) basis set. The total dipole moment ( $\mu_{\text{tot}}$ ) was calculated using the diagonal elements in equation (1). Similarly, equations (2) and (3) were also used to calculate average polarizability ( $\alpha$ ) and first hyperpolarizability ( $\beta_{\text{tot}}$ ), respectively. The calculated values for total dipole moment, average polarizability, and first hyperpolarizability for the chromophores Z1, Z2, Z3, and Z4 are presented in **Tables 6**.

**Table 6.** The dipole moments  $\mu$ , average isotropic polarizability  $\langle\alpha\rangle$  and the first hyperpolarizability  $\beta_{\text{tot}}$  of Z1-Z4

| Parameters                   | Z1              | Z2               | Z3               | Z4               |
|------------------------------|-----------------|------------------|------------------|------------------|
| $\mu_x$                      | 8.98            | 11.64            | -10.95           | -10.18           |
| $\mu_y$                      | -3.24           | 1.73             | -1.32            | -2.70            |
| $\mu_z$                      | -0.60           | -0.02            | 0.21             | 0.23             |
| $\mu_{\text{tot}}(D)$        | 9.56            | 11.77            | 11.03            | 10.54            |
| $\alpha_{xx}$                | 1711.91         | 3392.92          | 3344.28          | 2718.41          |
| $\alpha_{xy}$                | -54.32          | 46.34            | 107.13           | 112.52           |
| $\alpha_{yy}$                | 436.54          | 499.47           | 495.85           | 481.86           |
| $\alpha_{xz}$                | -47.72          | -51.21           | 41.99            | 23.61            |
| $\alpha_{yz}$                | 19.96           | 26.28            | -50.58           | -20.36           |
| $\alpha_{zz}$                | 188.17          | 232.84           | 253.97           | 210.40           |
| $\langle\alpha\rangle$ (a.u) | <b>778.87</b>   | <b>1375.07</b>   | <b>1364.70</b>   | <b>1136.89</b>   |
| $\beta_{xxx}$                | 89128.40        | -782688.00       | 517710.00        | -386020.0        |
| $\beta_{xxy}$                | 10191.80        | -35215.60        | 15295.70000      | -9856.18         |
| $\beta_{xyy}$                | -1000.82        | -1808.58         | 346.19700        | 1297.90          |
| $\beta_{yyy}$                | 460.77          | -298.30600       | 214.55400        | 60.20            |
| $\beta_{xxz}$                | -1116.45        | -2436.17000      | -5862.05         | -4671.27         |
| $\beta_{xyz}$                | -368.07         | -141.85400       | -2.62            | -290.27          |
| $\beta_{yyz}$                | 95.13           | 27.77490         | 17.75            | 44.14            |
| $\beta_{xzz}$                | -87.87          | -179.37600       | 47.72            | 117.06           |
| $\beta_{yzz}$                | -28.49          | -18.92280        | -35.39           | 8.98             |
| $\beta_{zzz}$                | 10.95           | 2.08982          | -0.79            | 2.06             |
| $\beta_{\text{tot}}$ (a.u)   | <b>88684.17</b> | <b>785483.75</b> | <b>518367.92</b> | <b>384757.33</b> |

As shown in **Table 6**, the linear polarizability results indicate that the polarizability tensor is along the x-axis is more dominant in all examined chromophores. According to the literature reviews, the energy difference between HOMO and

LUMO affects a molecule's polarizability. Chromophore with a small energy gap value has large linear polarizability.<sup>44</sup> This statement is applicable for our investigated systems, where Z2 exhibits the highest linear polarizability value of 1375.07 a.u. and Z1 presents the lowest linear polarizability value of 778.87 a. u. Z3 and Z4 polarizability values were 1364.70 a. u and 1136.89 a. u, respectively. Indeed, the decreasing order of linear polarizability values  $Z2 > Z3 > Z4 > Z1$  is found to be in reverse of energy gap order  $Z2 < Z3 < Z4 < Z1$ . In the case of first hyperpolarizability ( $\beta_{tot}$ ), the dominant contribution to  $\beta_{tot}$  is made by x-axis direction transition with positive values (89128.40, 517710.00 a. u) in Z1 and Z3, while with negative value (-782688.00, -386020.0 a. u) in Z2 and Z4, respectively. Generally, larger hyperpolarizability values are shown by chromophores with a small energy gap. This statement also exists in our studied systems where Z1, Z2, Z3, and Z4 presented the highest 88684.17, 785483.75, 518367.92, and 384757.33 a.u, respectively. Indeed, the decreasing order of  $\beta_{tot}$  values  $Z2 > Z3 > Z4 > Z1$  is discovered to correspond to the decreasing order of linear polarizability values  $Z2 > Z3 > Z4 > Z1$  and to the opposite order of energy gap values  $Z2 < Z3 < Z4 < Z1$ , respectively. In summary, the greatest  $\beta_{tot}$  values observed for the examined chromophores might be a consequence of the modification of various  $\pi$ -conjugated spacers. It can be noted that the NLO values of all compounds exceed those of the urea molecule, which is typically utilized as the organic molecule of reference ( $\beta_{tot}$  value of urea = 43 a. u).<sup>45</sup> Overall, the results imply that all compounds studied exhibit polarizable properties.

### 3.8 Absorption properties

To assess the effect of the solvent on the absorption spectra of chromophore Z1-Z4, various solvents with different polarities were employed. The TD-DFT computations at CAM-B3LYP/6-31G (*d,p*)<sup>46,47</sup> have been performed. The transition energy ( $E_{ex}$ ), oscillator strength ( $f$ ), transition natures, maximum absorption wavelength ( $\lambda_{max}$ ) of chromophore Z1-Z4 are summarized in Table 7, whereas absorption spectra of Z1-Z4 are displayed in fig. 6. According to Table 7 and fig. 6, the theoretical results suggest that the absorption wavelength values of Z1, Z2, and Z4 ranges from 567.84 to 593.30 nm, while the absorption wavelength values of Z3 range from 638.89 to 646.45 nm in the solvents studied. In addition, the  $S_0 \rightarrow S_1$  excitations of the chromophores Z1-Z4 having the oscillator strength between 2.23–2.80 are mainly contributed to HOMO  $\rightarrow$  LUMO transitions (85%, 50%, 62%, and 68%, respectively). We note that TD-DFT results suggest that there was no influence of solvent polarity on the absorption of chromophores Z1-Z4.

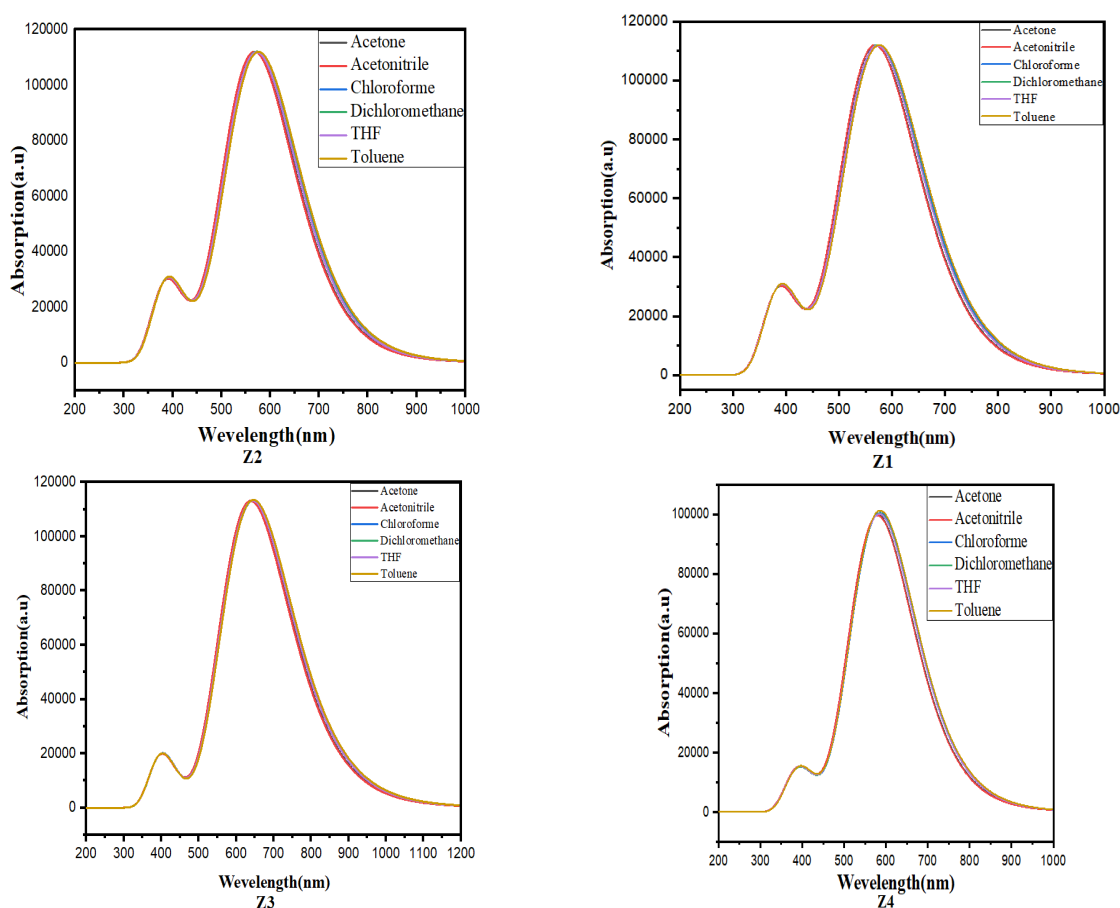


**Fig. 6.** UV-vis spectrum of four chromophores Z1-Z4 in various solvents

**Table 7.** Absorption spectra data obtained at TD-DFT/ CAM-B3LYP/6-31G (*d,p*) level.

| Chromophore | Solvent         | $\lambda_{\text{max}}(\text{nm})$ | $E_{\text{ex}}(\text{eV})$ | $f$  | MO/character | (%)   |
|-------------|-----------------|-----------------------------------|----------------------------|------|--------------|-------|
| Z1          | Acetone         | 590.11                            | 2.10                       | 2.23 | HOMO->LUMO   | (85%) |
|             | Acetonitrile    | 589.41                            | 2.10                       | 2.23 | HOMO->LUMO   | (85%) |
|             | Chloroform      | 574.58                            | 2.15                       | 2.75 | HOMO->LUMO   | (85%) |
|             | Dichloromethane | 593.30                            | 2.08                       | 2.24 | HOMO->LUMO   | (85%) |
|             | THF             | 591.38                            | 2.09                       | 2.23 | HOMO->LUMO   | (85%) |
|             | Toluene         | 588.71                            | 2.10                       | 2.24 | HOMO->LUMO   | (85%) |
| Z2          | Acetone         | 568.93                            | 2.17                       | 2.76 | HOMO->LUMO   | (50%) |
|             | Acetonitrile    | 567.84                            | 2.18                       | 2.76 | HOMO->LUMO   | (50%) |
|             | Chloroform      | 574.58                            | 2.15                       | 2.75 | HOMO->LUMO   | (50%) |
|             | Dichloromethane | 572.80                            | 2.16                       | 2.76 | HOMO->LUMO   | (50%) |
|             | THF             | 572.30                            | 2.16                       | 2.76 | HOMO->LUMO   | (50%) |
|             | Toluene         | 576.26                            | 2.15                       | 2.76 | HOMO->LUMO   | (50%) |
| Z3          | Acetone         | 640.17                            | 1.91                       | 2.79 | HOMO->LUMO   | (62%) |
|             | Acetonitrile    | 638.89                            | 1.94                       | 2.79 | HOMO->LUMO   | (62%) |
|             | Chloroform      | 645.98                            | 1.91                       | 2.79 | HOMO->LUMO   | (62%) |
|             | Dichloromethane | 644.80                            | 1.92                       | 2.79 | HOMO->LUMO   | (62%) |
|             | THF             | 643.70                            | 1.92                       | 2.79 | HOMO->LUMO   | (62%) |
|             | Toluene         | 646.45                            | 1.91                       | 2.80 | HOMO->LUMO   | (62%) |
| Z4          | Acetone         | 581.26                            | 2.13                       | 2.46 | HOMO->LUMO   | (68%) |
|             | Acetonitrile    | 580.09                            | 2.13                       | 2.45 | HOMO->LUMO   | (68%) |
|             | Chloroform      | 586.43                            | 2.11                       | 2.48 | HOMO->LUMO   | (68%) |
|             | Dichloromethane | 586.26                            | 2.11                       | 2.50 | HOMO->LUMO   | (68%) |
|             | THF             | 584.49                            | 2.12                       | 2.47 | HOMO->LUMO   | (68%) |
|             | Toluene         | 586.26                            | 2.11                       | 2.50 | HOMO->LUMO   | (68%) |

#### 4. Conclusion

This study designed a series of organic chromophores (Z1-Z4) based on benzoxazine as the electron donor (D) and tricyanovinyl dihydrofuran (TCF) as the electron acceptor (A) having D- $\pi$ -A architecture and explored the potential effect of  $\pi$ -spacers (bridges) on their NLO properties. All designed organic compounds showed maximum wavelengths  $\lambda_{\text{max}}$  in the visible region with small transition energy values. FMO analysis of Z1 to Z4 indicated that energy band gaps of the entitled chromophores were reduced from 1.15 eV to 0.79 eV. Their NBO charge analysis indicates that electrons could effectively migrate from donor to acceptor through  $\pi$ -spacers, resulting in a high charge separation state. Generally, all dyes (Z1-Z4) present a large NLO response ranging from 88684.17 to 785483.75 (a.u.), Z2 especially presents the highest  $\langle a \rangle$  [(1375.07 (a.u.)) and  $\beta_{\text{tot}}$  (785483.75(a.u.)) values. The studied chromophores exhibited good NLO properties because of their  $\beta$  values and were much greater than that of urea. The polarizability and hyperpolarizabilities parameters of the chromophores studied indicate that they are accomplished candidates for NLO material.

#### References

- Costes J. P., Lamère J. F., Lepetit C., Lacroix P. G., Dahan F., & Nakatani K. (2005) Synthesis, Crystal Structures, and Nonlinear Optical (NLO) Properties of New Schiff-Base Nickel(II) Complexes. Toward a New Type of Molecular Switch. *Inorg Chem.*, 44 (6) 1973-1982.
- Santo D. B., & Fragalà I. (2000) Synthesis and second-order nonlinear optical properties of bis (salicylaldiminato) M (II) metalloorganic materials. *Synthetic Metals.*, 115 (1-3) 191-196.
- Lacroix P. G. (2001) second-Order Optical Nonlinearities in Coordination Chemistry: The Case of Bis (salicylaldiminato) metal Schiff Base Complexes. *Eur J Inorg Chem.*, 2001 (2) 339-348.
- Williams D. J. (1984) Organic Polymeric and Non-Polymeric Materials with Large Optical Nonlinearities. *Angew Chem Int Ed Engl.*, 23 (9) 690 -703.
- Janjua M. R. S. A. (2017) Nonlinear optical response of a series of small molecules: quantum modification of  $\pi$ -spacer and acceptor. *J Iran Cheme SOC.*, 14 (9) 2041-2054.
- Zhong R. L., Xu H. L., Li Z. R., & Su ZM. (2015) Role of Excess Electrons in Nonlinear Optical Response. *J Phys Chem Lett.*, 6 (4) 612-619.
- Muhammad S., Xu H. L., Zhong R. L., Su Z. M., Al-Sehemi A. G., & Irfan A. (2013) Quantum chemical design of nonlinear optical materials by sp<sup>2</sup>-hybridized carbon nanomaterials: issues and opportunities. *J Mater Chem C.*, 1 (35) 5439.
- Garza A. J., Osman O. I., Wazzan N. A., Khan S. B., Asiri A. M., and Scuseria G. E. (2014) A computational study of the nonlinear optical properties of carbazole derivatives: theory refines experiment. *Theor Chem Acc.*, 133 (4) 1458.
- Janjua M. R. S. A., Amin M., Ali M., Bashir B., Khan M. U., Iqbal M. A., Guan W., Yan L., and Su Z. M (2012) A DFT Study on The Two-Dimensional Second-Order Nonlinear Optical (NLO) Response of Terpyridine-Substituted Hexamolybdates: Physical Insight on 2D Inorganic-Organic Hybrid Functional Materials. *Eur J Inorg Chem.*, 2012 (4) 705-711.
- Dalton L. (2002) Nonlinear Optical Polymeric Materials: From Chromophore Design to Commercial Applications. *Advances in Polymer Science.*, 158 1-86.



- 11 Dulcic A., Flytzanis C., Tang C. L., Pépin D., Fétizon M., & Hoppilliard Y. (1981) Length dependence of the second-order optical nonlinearity in conjugated hydrocarbons. *The Journal of Chemical Physics.*, 74 (3) 1559-1563.
- 12 Zyss J., & Ledoux I. (1994) Nonlinear optics in multipolar media: theory and experiments. *Chem Rev.*, 94 (1) 77-105.
- 13 Entwistle C. D., Collings J. C., Steffen A., Palsson L. O., Beeby A., Jove D. A., Burke J. M., Batsanov A S., Howard J. A. K., Mosely J. A., Poon S. Y., Wo W. Y., Ibersiene F., Fathallah S., Boucekkine A., Halet J. F. O., & Marder T. B. (2009) Syntheses, structures, two-photon absorption cross-sections and computed second hyperpolarisabilities of quadrupolar A- $\pi$ -A systems containing E-dimesitylborylethenyl acceptors. *J Mater Chem.*, 19 (40) 7532-7544.
- 14 Wang H., Zhang M., Yang Y., Liu F., Hu C., Xiao H., Qiu L., Liu X., Liu J., & Zhen Z. (2016) Synthesis and characterization of one novel second-order nonlinear optical chromophore based on new benzoxazin donor. *Materials Letters.*, 164 644 - 646.
- 15 Becke A. D. (1988) Density-functional exchange-energy approximation with correct asymptotic behavior. *Phys Rev A.*, 38 (6) 3098-3100.
- 16 Lee C., Yang W., & Parr R. G. (1988) Development of the Colle-Salvetti correlation-energy formula into a functional of the electron density. *Phys Rev B.*, 37 (2) 785-789.
- 17 Perdew J. P., Burke K., & Ernzerhof M. (1996) Generalized Gradient Approximation Made Simple. *Phys Rev Lett.*, 77 (18) 3865-3868.
- 18 Govindarajan M., Ganesan K., Periandy S., and Mohan S. (2010) DFT (LSDA, B3LYP and B3PW91) comparative vibrational spectroscopic analysis of -acetonephthone. *Inorganica Chimica Acta.*, 486 162-171.
- 19 Adamo C., & Barone V. (1998) Exchange functionals with improved long-range behavior and adiabatic connection methods without adjustable parameters: The mPW and mPW1PW models. *The Journal of Chemical Physics.*, 108 (2) 664-675.
- 20 Stratmann R. E., Scuseria G. E., & Frisch M J. (1998) An efficient implementation of time-dependent density-functional theory for the calculation of excitation energies of large molecules. *The Journal of Chemical Physics.*, 109 (19) 8218-8224.
- 21 Casida M. E., Jamorski C., Casida K. C., & Salahub D. R. (1998) Molecular excitation energies to high-lying bound states from time-dependent local density approximation ionization threshold. *The Journal of Chemical Physics.*, 108 (11) 4439-44
- 22 Frisch C. J., Trucks G. W., Schlegel H. B., Scuseria G. E., Robb M. A., et al, (2009) Gaussian 09, Revision A.02.
- 23 Kumer A., Chakma, U., Matin M. M., Akash S., Chando A., & Howlader D. (2021) The computational screening of inhibitor for black fungus and white fungus by D-glucofuranose derivatives using in silico and SAR study. *Org. Commun.*, 14 (4) 305-322.
- 24 Islam N., Islam M. D., Rahman M. R., & Matin M. M. (2021) Octyl 6-O-hexanoyl- $\beta$ -D-glucopyranosides: Synthesis, PASS, antibacterial, in silico ADMET, and DFT studies. *Curr. Chem. Lett.*, 10 (4) 413-426.
- 25 Haneef U., Rahman M. R., & Matin M. M. (2021) Synthesis, PASS, in silico ADMET, and thermodynamic studies of some galactopyranoside esters. *Phys. Chem. Res.*, 9 (4) 591-603.
- 26 Foster J. P., and Weinhold F. (1980) Natural hybrid orbitals. *J Am Chem Soc.*, 102 (24) 7211-7218.
- 27 Guillaumont D., & Nakamura S. (2000) Calculation of the absorption wavelength of dyes using time-dependent density-functional theory (TD-DFT). *Dyes and Pigments.*, 46( 2) 85-92.
- 28 Yanai T., Tew D. P., & Handy N. C. (2004) A new hybrid exchange-correlation functional using the Coulomb-attenuating method (CAM-B3LYP). *Chemical Physics Letters.*, 393(1-3) 51-57.
- 29 Lin C., & Wu K. (2000) Theoretical studies on the nonlinear optical susceptibilities of 3-methoxy-4-hydroxy-benzaldehyde crystal. *Chemical Physics Letters.*, 321 (1-2) 83-88.
- 30 Karamanis P., Pouchan C., & Maroulis G. (2008) Structure, stability, dipole polarizability and differential polarizability in small gallium arsenide clusters from all-electron ab initio and density-functional-theory calculations. *Phys Rev A.*, 77 (1) 013201.
- 31 Ghanavatkari C. W., Mishra V. R., & Sekar N. (2021) Review of NLO phoric azo dyes – Developments in hyperpolarizabilities in last two decades. *Dyes and Pigments.*, 191 109367.
- 32 Kacimi R., Bourass M., Toupance T., Wazzan N., Chemek M., El Alamy A., Bejjit L., Alimi K., & Bouachrine M. (2020) Computational design of new organic (D- $\pi$ -A) dyes based on benzothiadiazole for photovoltaic applications, especially dye-sensitized solar cells. *Res Chem Intermed.*, 46 (6) 3247-3262.
- 33 Etabti H., Fitri A., Benjelloun A. T., Hachi M., Benzakour M., & Mcharfi M. (2021) Benzocarbazole-based D-Di- $\pi$ -A dyes for DSSCs: DFT/TD-DFT study of influence of auxiliary donors on the performance of free dye and dye-TiO<sub>2</sub> interface. *Res Chem Intermed.*, 47 (10) 4257-4280.
- 34 Rajan V. K., & Muraleedharan K. (2017) A computational investigation on the structure, global parameters and antioxidant capacity of a polyphenol, *Gallic acid*. *Food Chemistry.*, 220 93-99.
- 35 Daolio A., Pizzi A., Calabrese M., Terraneo G., Bordignon S., Frontera A., & Resnati, V. (2021) Molecular Electrostatic Potential and Noncovalent Interactions in Derivatives of Group 8 Elements. *Zitierweise: Angew. Chem. Int. Ed.*, 60 (133) 20723 - 20727.
- 36 Wang H, Wang X, Wang H, Wang L, & Liu A. (2007) DFT study of new bipyrazole derivatives and their potential activity as corrosion inhibitor. *J Mol Model.*, 13 147-153.
- 37 Raftani M., Abram T., Loued W., Kacimi R., Azaid A., Alimi K., Bennani M. N., & Bouachrine M. (2021) The optoelectronic properties of  $\pi$ -conjugated organic molecules based on terphenyl and pyrrole for BHJ solar cells: DFT / TD-DFT theoretical study. *Current Chemistry Letters.*, 10 (4) 489-502.

- 38 Islam N., & Ghosh D. C. (2012) On the Electrophilic Character of Molecules Through Its Relation with Electronegativity and Chemical Hardness. *International Journal of Molecular Sciences.*, 13 2160-2175.
- 39 Parr R. G., & Pearson R. G. (1983) Absolute hardness: companion parameter to absolute electronegativity. *J Am Chem Soc.*, 105 (26) 7512-7516.
- 40 Parr R. G., Donnelly R. A., Levy M., & Palke W. E. (1978) Electronegativity: The density functional view point. *The Journal of Chemical Physics.*, 68 (8) 3801-3807.
- 41 Aziz S. G., Elroby S. A. K., Hilal R. H., & Osman O. I. (2014) Theoretical and computational studies of conformation, natural bond orbital and nonlinear optical properties of cis-N-phenylbenzohydroxamic acid. *Computational and Theoretical Chemistry.*, 1028 65-71.
- 42 Peng Z., & Yu L. (1994) Second-Order Nonlinear Optical Polyimide with High-Temperature Stability. *Macromolecules.*, 27 (9) 2638-2640.
- 43 Tsutsumi N., Morishima M., & Sakai W. (1998) Nonlinear Optical (NLO) Polymers. 3. NLO Polyimide with Dipole Moments Aligned Transverse to the Imide Linkage. *Macromolecules.*, 31 (22) 7764-7769.
- 44 Hussain A., Khan M. U., Ibrahim M., Khalid M., Ali A., Hussain S., Saleem M., Ahmad N., Muhammad S., Al-Sehemi A G., & Sultan A. (2020) Structural parameters, electronic, linear and nonlinear optical exploration of thiopyrimidine derivatives: A comparison between DFT/TDDFT and experimental study. *Journal of Molecular Structure.*, 1201 127-183.
- 45 Jawaria R., Hussain M., Khalid M., Khan U. M., Tahir N. M., Naseer M. M., Braga C. A. A., & Shafiq Z. (2019) Synthesis, crystal structure analysis, spectral characterization and nonlinear optical exploration of potent thiosemicarbazones based compounds: A DFT refine experimental study. *Inorganica Chimica Acta.*, 486 162-171.
- 46 Zaitri L. K., & Mekelleche S. M. (2021) DFT and TD-DFT Study on Quadratic NLO Response and Optoelectronic Activity in Novel Y-Shaped Imidazole-Based Push-Pull Chromophores. *In Review.*, 136 (27) 1-14.
- 47 Khalid M., Khan M. U., Shafiq I., Hussain R., Mahmood K., Hussain A., Jawaria R., Hussain A., Imran M., Assiri M. A., Ali A., Rehman M. F. U., Sun K., & Li Y. (2021) NLO potential exploration for D- $\pi$ -A heterocyclic organic compounds by incorporation of various  $\pi$ -linkers and acceptor units. *Arabian Journal of Chemistry.*, 14 (8) 1878-5352.



© 2022 by the authors; licensee Growing Science, Canada. This is an open access article distributed under the terms and conditions of the Creative Commons Attribution (CC-BY) license (<http://creativecommons.org/licenses/by/4.0/>).